JGR Planets

RESEARCH ARTICLE
10.1029/2021JE006952

The Effects of Planetary and Stellar Parameters on Brittle Lithospheric Thickness

Paul K. Byrne[1,2], Bradford J. Foley[3], Marie E. S. Violay[4], Michael J. Heap[5,6], and Sami Mikhail[7]

[1]Department of Marine, Earth, and Atmospheric Sciences, North Carolina State University, Raleigh, NC, USA, [2]Department of Earth and Planetary Sciences, Washington University in St. Louis, St. Louis, MO, USA, [3]Department of Geosciences, Pennsylvania State University, University Park, PA, USA, [4]Laboratory of Experimental Rock Mechanics EPFL, Lausanne, Switzerland, [5]Université de Strasbourg, CNRS, Institut Terre et Environnement de Strasbourg, Strasbourg, France, [6]Institut Universitaire de France, Paris, France, [7]The School of Earth and Environmental Sciences, The University of St Andrews, Scotland, UK

Key Points:

- We modeled the effects of planetary mass, age, and surface temperature on brittle lithospheric thickness
- Surface temperature is the primary determinant of the thickness of brittle exoplanet lithospheres
- Certain combinations of these parameters yield "eggshell planets"—worlds with ultra-thin brittle lithospheres

Supporting Information:

Supporting Information may be found in the online version of this article.

Correspondence to:

P. K. Byrne,
paul.byrne@wustl.edu

Citation:

Byrne, P. K., Foley, B. J., Violay, M. E. S., Heap, M. J., & Mikhail, S. (2021). The effects of planetary and stellar parameters on brittle lithospheric thickness. *Journal of Geophysical Research: Planets*, *126*, e2021JE006952. https://doi.org/10.1029/2021JE006952

Received 10 MAY 2021
Accepted 12 OCT 2021

Author Contributions:

Conceptualization: Paul K. Byrne, Michael J. Heap, Sami Mikhail
Formal analysis: Paul K. Byrne, Bradford J. Foley
Investigation: Paul K. Byrne, Bradford J. Foley, Marie E. S. Violay, Michael J. Heap, Sami Mikhail
Methodology: Paul K. Byrne, Bradford J. Foley, Michael J. Heap, Sami Mikhail
Supervision: Paul K. Byrne
Validation: Marie E. S. Violay
Visualization: Paul K. Byrne, Bradford J. Foley, Marie E. S. Violay
Writing – original draft: Paul K. Byrne, Bradford J. Foley, Marie E. S. Violay, Michael J. Heap, Sami Mikhail
Writing – review & editing: Paul K. Byrne, Bradford J. Foley, Marie E. S. Violay, Michael J. Heap, Sami Mikhail

Abstract The thickness of the brittle lithosphere—the outer portion of a planetary body that fails via fracturing—plays a key role in the geological processes of that body. The properties of both a planet and its host star can influence that thickness, and the potential range of those properties exceeds what we see in the Solar System. To understand how planetary and stellar parameters influence brittle lithospheric thickness generally, we modeled a comprehensive suite of combinations of planetary mass, surface and mantle temperature, heat flux, and strain rate. Surface temperature is the dominant factor governing the thickness of the brittle layer: smaller and older planets generally have thick brittle lithospheres, akin to those of Mercury and Mars, whereas larger, younger planets have thinner brittle lithospheres that may be comparable to the Venus lowlands. But certain combinations of these parameters yield worlds with exceedingly thin brittle layers. We predict that such bodies have little elevated topography and limited volatile cycling and weathering, which can be tested by future telescopic observations of known extrasolar planets.

Plain Language Summary The outer layer of a rocky planetary body is generally rigid and behaves in a brittle manner. The thickness of this layer is important in governing numerous aspects of that body's geological character, including whether it can support plate tectonics and even retain habitable conditions at the surface. Factors inherent to the planet, such as size, interior temperature, composition, and even climate affect the thickness of this outer layer, but so too do factors specific to the host star, including how luminous and far away it is. We ran a large set of computer models to see how various combinations of planetary and stellar properties influence the thickness of a planetary body's outer layer. Our models predict that worlds that are small, old, or far from their star likely have thick, rigid layers but, in some circumstances, planets might have an outer brittle layer only a few kilometers thick. These worlds, which we call "eggshell planets," might resemble the lowlands on Venus, and we suggest that at least three such extrasolar planets are already known. We propose that these planets be examined with planned and future space telescopes to test if our models are correct.

1. Introduction

The outermost portion of a solid planetary body is termed the lithosphere (e.g., Phillips et al., 1997). The lithosphere usually comprises a relatively cold, upper portion where brittle deformation dominates, and a relatively warm, lower region that responds to stress in a ductile manner (e.g., Kohlstedt & Mackwell, 2010). In the brittle lithosphere, tectonic deformation is accomplished by localized fracturing processes, commonly forming shear fractures (i.e., faults), before giving way to semi-brittle deformation (i.e., both localized frictional sliding and bulk deformation) with increasing depth. At yet greater temperatures and pressures, deformation is primarily accommodated by distributed plastic flow mechanisms such as dislocation glide or diffusion creep (e.g., Kohlstedt et al., 1995). The zone in the lithosphere where the dominantly brittle behavior changes to dominantly ductile deformation is termed the brittle-ductile transition (BDT, also referred to as the brittle-plastic transition), and is dependent on a variety of factors including temperature, pressure, strain rate, composition, grain size, and the presence of fluid (Kohlstedt et al., 1995; Violay et al., 2012). On

Earth, the brittle lithosphere typically encompasses the crust and the uppermost lithospheric mantle, with the mantle below that portion constituting the main component of the ductile lithosphere.

The strength of the brittle lithosphere, which can be taken as a function of its thickness (Comer et al., 1985), is a key component of a planetary body's geological character and evolution and influences how, for example, surface loads are accommodated (Solomon & Head, 1980), surface tectonism is manifest (Beuthe, 2010; Byrne et al., 2014), interior heat is lost to space (e.g., Stern et al., 2018), and even how any atmosphere present is degassed and sustained (Mikhail & Heap, 2017). However, in the absence of in situ investigation, the depth of the transition from brittle to ductile deformation within a planetary body can be estimated by forward modeling of the penetration depths of tectonic structures (Egea-González et al., 2012; Peterson et al., 2020), matching models of flexural induced strains to geological observations (e.g., Solomon & Head, 1980), studies of topography–gravity admittance and correlation spectra (McGovern et al., 2002, 2004; Turcotte et al., 1981), and computed lithospheric strength profiles (Katayama, 2021; Klimczak et al., 2019; Suppe & Connors, 1992).

Placing estimates on BDT depth for planetary bodies beyond Earth thus ideally requires remotely sensed image, topographic, geophysical, and compositional data. Yet making such estimates for rocky planets in orbit about other stars is even more challenging, given that very little geological information is available for these worlds. Even so, it is important to understand the mechanical characteristics of planetary lithospheres when predicting the coupled geological and environmental conditions of extrasolar planets. For example, the degree to which plate tectonics can operate on super-Earths remains unclear (Korenaga, 2010, 2017; O'Neill & Lenardic, 2007; Stein et al., 2011; Valencia et al., 2007; van Heck & Tackley, 2011), especially considering that brittle layer thickness is a key parameter for establishing lithospheric strength in plate tectonics models (O'Neill et al., 2007; Stern et al., 2018; Valencia et al., 2007). Placing bounds on brittle lithosphere thickness also helps establish strain portioning between frictional sliding on faults and bulk deformation via plastic processes in controlling lithospheric strength and the formation of plate boundaries (e.g., Foley et al., 2012; Korenaga, 2020; Montési, 2013; Mulyukova & Bercovici, 2017).

Importantly, the possible value ranges of the parameters that control BDT depth extend beyond those we see in the Solar System. Surface gravitational acceleration, with consequent implications for where pressure becomes sufficiently high to facilitate ductile deformation, is greater on super-Earths than on any rocky body in the Solar System. Similarly, interior heat flux as a function of planetary age, radiogenic element abundance, or both, vary for planetary systems that are older than our own (e.g., Kepler-444: Campante et al., [2015]) or that have different starting compositions (e.g., where Si/Al, Fe/Mg, or K/U ratios deviate from chondritic values). And planetary surface temperatures can plausibly exceed those of Mercury or Venus without approaching rock liquidi (cf. 55 Cancri e: Demory et al., 2011), whether because of proximity to host star (and thus incident stellar radiation), greenhouse conditions as a function of volatile element enrichment (such as C/O, S/O, etc.), or both.

In this study, we aim to better understand how the confluence of several major planetary properties—mass, surface temperature, mantle interior temperature, and heat flux—together influences the thickness of brittle lithospheres generally, for a range of input values greater than but encompassing those of the terrestrial planets in the Solar System. We describe an analytical approach to calculate brittle lithospheric thickness for combinations of these values and assess what factor(s) plays a leading role in determining this thickness. We then discuss our results in the context of several known super-Earth exoplanets.

2. Methods

To calculate the depth of the brittle-ductile transition as a function of planetary mass, surface temperature, and heat flux (which we take as "plate age"), we considered a planet with a basaltic crust and peridotitic mantle, assuming that brittle lithospheric strength is given by the minimum differential stress needed for frictional sliding along fractures (Byerlee, 1978), and that stress needed for driving viscous flow at a specified strain rate (e.g., Kohlstedt et al., 1995). Here, plate age refers to an effective cooling age of the lithosphere, with the lithospheric temperature profile governed by an error function; this effective cooling age then sets the ultimate thickness of the whole (brittle-plus-ductile) lithosphere for a planet with plate tectonics. We followed the formulation of Kohlstedt et al. (1995) in calculating brittle strength. Specifically,

Amonton's Law gives the shear stress required for frictional sliding, τ, as a function of the effective normal stress on the fault, $\sigma_n - \alpha P_f$,

$$T = C_f + \mu_f \left(\sigma_n - \alpha P_f\right) \quad (1)$$

where C_f is frictional cohesive strength μ_f is the static coefficient of friction, σ_n is the normal stress, α is a constant (of order unity, and taken here as 1), and P_f is pore fluid pressure. For $\sigma_n < 200$ MPa, $\mu_f \approx 0.85$ and $C_f = 0$, whereas for $\sigma_n > 200$ MPa, $\mu_f \approx 0.6$, and $C_f \approx 60$ MPa (Byerlee, 1978). For a thrust fault with a dip angle of 60°, where the maximum principal compressive stress, σ_1, is in the horizontal plane and the minimum principal compressive stress, σ_3, is vertical, Equation 1 becomes

$$\sigma_1 - P_f = 4.9\left(\sigma_3 - P_f\right) \quad (2)$$

for $\sigma_3 - P_f < 100$ MPa. For $\sigma_3 - P_f > 100$ MPa, we use the relation

$$\sigma_1 - P_f = 3.1\left(\sigma_3 - P_f\right) + 210 \quad (3)$$

The vertical stress is given by $\sigma_3 = \rho g z$, where ρ is bulk rock density, g is surface gravitational acceleration, and z is depth; here, $P_f = \rho_f g z$, where ρ_f is the fluid density. Strength is then defined as the differential stress, σ, along the fault—that is, $\sigma_1 - \sigma_3$. When plotting strength profiles for Earth, we assumed hydrostatic fluid pressure; we also ran some sets of models for exoplanets incorporating hydrostatic pore pressure, to test the influence of P_f. In most cases, however, we assumed that $P_f = 0$ because we consider exoplanets of a variety of sizes and with a broad range of surface temperatures, such that the presence of a pressurized fluid phase (of whatever chemistry and provenance) cannot be assured.

To calculate the stress needed to induce viscous flow, we employed a composite rheological behavior consisting of dislocation creep and low-temperature plasticity. We found that the contribution to mid- or lower-lithospheric flow from diffusion creep is negligible at the stresses seen in our calculations, using flow-law formulations and parameters from Hirth and Kohlstedt (2003). Diffusion creep (or grain boundary sliding) could be an important creep mechanism at plate boundaries, should grain-size reduction be substantial there (e.g., Warren & Hirth, 2006). However, our calculations are aimed at capturing the strength and structure of the typical lithosphere, away from plate boundaries.

Frictional strength is dependent on fault orientation and stress state, but largely insensitive to lithology (Byerlee, 1978), so Equation 1 holds regardless of whether we consider crustal or mantle material that fails in a brittle manner. Lithology substantially influences the flow laws for solid-state creep, however. As stated above, we assumed that peridotite (olivine-orthopyroxene-clinopyroxene) is the dominant lithology, as is the case for oceanic lithosphere on Earth, and hence used peridotite flow laws in our calculations. This choice is justified by the observation of widespread basaltic volcanism on inner Solar System bodies (Byrne, 2019; Head & Wilson, 1992; Strom et al., 1975; Surkov et al., 1983; Tanaka et al., 2014) and perhaps even on exoplanets (e.g., Kreidberg et al., 2019), which is consistent with being sourced from a peridotitic mantle source (Yoder & Tilley, 1962).

However, for very shallow BDT zones, where this transition would reside in the crust, BDT depth is likely overestimated in our models. For a peridotitic mantle and basaltic crust as assumed here, crustal material will be weaker than the mantle in terms of viscous flow. As a result, utilizing a flow law for basalt would result in even shallower BDT depths than our calculations show (Violay et al., 2012). In addition, for crusts that are very thick (e.g., tens of km), it is possible for there to be two BDT zones present—one in the crust, and a second in the mantle. Such a mechanical arrangement results in a weak, viscous lower crust sitting atop a strong, brittle "lithospheric" mantle, a crustal strength profile that has been argued for continental settings on Earth (e.g., Kohlstedt & Mackwell, 2010). Our decision to not use a flow law for crustal material, considering instead only mantle rheology for ductile deformation, means that our calculated BDT depth values are maxima.

Flow laws describing ductile rock behavior are derived from experimental studies of the brittle and ductile domains, which yield simple constitutive equations meant to describe deformation by a single mechanism (Kohlstedt et al., 1995). The flow law for dislocation creep (e.g., Hirth & Kohlstedt, 2003) is given by:

$$\dot{\varepsilon}_{dis} = A_{dis} \exp\left(-\frac{E_{dis} + PV_{dis}}{RT}\right)\sigma^{n} \tag{4}$$

where $\dot{\varepsilon}_{dis}$ is strain rate due to dislocation creep, A_{dis} is a constant, E_{dis} is the activation energy for dislocation creep, V_{dis} is the activation volume for dislocation creep, R is the universal gas constant, T is temperature, and n is the stress exponent, which is a constant. We used values from Hirth and Kohlstedt (2003) of $A_{dis} = 1.1 \times 10^{5}$ s^{-1} MPa^{-n}, $E_{dis} = 520$ kJ mol^{-1}, $V_{dis} = 10^{-6}$ m^3 mol^{-1}, $R = 8.314$ J mol^{-1} K^{-1}, and $n = 3.5$, although there is still considerable uncertainty in the olivine flow law and its parameters (Jain et al., 2019; Jain & Korenaga, 2020).

The flow law for low-temperature plasticity is not well established (e.g., Demouchy et al., 2013; Kumamoto et al., 2017). Even so, Jain et al. (2017) were able to invert for flow law parameters by fitting to a large suite of rock mechanics experimental data a generic, low-temperature plasticity flow law of the form:

$$\dot{\varepsilon}_{lt} = A_{lt}\sigma^{2} exp\left(-\frac{E_{lt} + PV_{lt}}{RT}\left[1 - \left\{\frac{\sigma}{\sigma_{p}}\right\}^{p}\right]^{q}\right) \tag{5}$$

where $\dot{\varepsilon}_{lt}$ is strain rate due to low-temperature plasticity, E_{lt} and V_{lt} are the activation energy and volume, respectively, for low-temperature plasticity, A_{lt}, p, and q are constants, and σ_p is the Peierls stress. Peierls stress, in turn (Jain et al., 2017), is a function of pressure such that

$$\sigma_{p} = \sigma_{p0}\left(1 + \frac{G'P}{G_{0}}\right) \tag{6}$$

where σ_{p0} is the Peierls stress at zero pressure, G' is the pressure derivative of the shear modulus, and G_0 is the shear modulus at zero pressure. The constants p and q depend on the shape of the Peierls function (Jain et al., 2017). We ran sets of models both with $p = 1$, $q = 2$, and with $p = 0.5$, $q = 2$. As we show in Section 3, the BDT is deeper when $p = 0.5$ and $q = 2$; we consider this case to be our baseline model, as it is more conservative for our investigation of planets with very thin brittle lithospheres. We used the median values from Jain et al. (2017) for our flow-law parameters. For $p = 0.5$ and $q = 2$, we used $A_{lt} = 1.7 \times 10^{-8}$ s^{-1} Pa^{-2}, $E_{lt} = 452$ kJ mol^{-1}, $V_{lt} = 8$ cm^3 mol^{-1}, and $\sigma_{p0} = 7.32$ GPa; for $p = 1$ and $q = 2$, we took $A_{lt} = 2.04 \times 10^{-8}$ s^{-1} Pa^{-2}, $E_{lt} = 225$ kJ mol^{-1}, $V_{lt} = 3$ cm^3 mol^{-1}, and $\sigma_{p0} = 6.2$ GPa. For all models, $G' = 1.61$ and $G_0 = 77.4 \times 10^{9}$ Pa.

To determine the geotherm through the lithosphere, we employed a classic half-space model of hot mantle cooling from above because of an imposed cooler surface temperature. The effective age of the lithosphere, t—that is, how long it has been cooling from above—along with the surface and mantle temperatures (T_s and T_m, respectively) then set the ultimate thickness of the lithosphere, and thus the surface heat flux. Following Turcotte and Schubert (2002), the geotherm is given by the relation

$$T(z) = T_S + (T_m - T_s)\,erf\left(\frac{z}{2\sqrt{\kappa t}}\right) \tag{7}$$

where κ is the thermal diffusivity ($\kappa \approx 10^{-6}$ m^2 s^{-1}). The total strain rate, $\dot{\varepsilon}$, is $\dot{\varepsilon}_{dis} + \dot{\varepsilon}_{lt}$. Fixing the strain rate, differential stress can then be solved as a function of depth, z, for viscous deformation. This stress increases sharply as z goes to zero because lower temperatures make rocks exponentially stiffer. The intersection of the stress needed for frictional sliding and that needed for viscous deformation then gives the point where it becomes easier to deform the bulk rock via plasticity rather than to slide on fault planes, that is, the base of the BDT zone and thus the greatest thickness of the brittle lithosphere.

Table 1
The Parameters and Assumed Values Used in Our Brittle-Ductile Transition Depth Calculations

Parameter	Symbol	Value	Equation	Reference
Surface gravity	g	5–40 m s^{-2}	(3)	
Surface temperature	T_s	200–1000 K	(7)	
Mantle interior temperature	T_m	1500–2000 K	(7)	
Lithospheric cooling age	T	5–300 Myr	(7)	
Strain rate	$\dot{\varepsilon}$	10^{-13}–10^{-16} s^{-1}	(4), (5)	Kohlstedt et al. (1995)
Lithosphere density	P	3500 kg m^{-3}	(3)	Kohlstedt et al. (1995)
Geometric constant	A	1	(1)	Kohlstedt et al. (1995)
Fluid density (assumed hydrostatic)	ρ_f	1000 kg m^{-3}	(3)	Kohlstedt et al. (1995)
Pre-exponential constant for dislocation creep	A_{dis}	1.1×10^5 s^{-1} MPa^{-n}	(4)	Hirth and Kohlstedt (2003)
Activation energy for dislocation creep	E_{dis}	520 kJ mol^{-1}	(4)	Hirth and Kohlstedt (2003)
Activation volume for dislocation creep	V_{dis}	10^{-6} m^3 mol^{-1}	(4)	Hirth and Kohlstedt (2003)
Universal gas constant	R	8.314 J mol^{-1} K^{-1}	(4)	Hirth and Kohlstedt (2003)
Stress exponent	N	3.5	(4)	Hirth and Kohlstedt (2003)
Pre-exponential constant for low-temperature plasticity	A_{lt}	1.7×10^{-8} s^{-1} Pa^{-2} for $p = 0.5$	(5)	Jain et al. (2017)
		2.04×10^{-8} s^{-1} Pa^{-2} for $p = 1$		
Activation energy for low-temperature plasticity	E_{lt}	452 kJ mol^{-1} for $p = 0.5$	(5)	Jain et al. (2017)
		225 kJ mol^{-1} for $p = 1$		
Activation volume for dislocation creep	V_{lt}	8 cm^3 mol^{-1} for $p = 0.5$	(5)	Jain et al. (2017)
		3 cm^3 mol^{-1} for $p = 1$		
Stress exponent	P	0.5 or 1	(5)	Jain et al. (2017)
Stress exponent	Q	2	(5)	Jain et al. (2017)
Peierls stress at zero pressure	σ_{p0}	7.32 GPa for $p = 0.5$	(5)	Jain et al. (2017)
		6.2 GPa for $p = 1$		
Shear modulus at zero pressure	G_0	77.4 GPa	(6)	Jain et al. (2017)
Pressure derivative of the shear modulus	G'	1.61	(6)	Jain et al. (2017)
Thermal diffusivity	κ	10^{-6} m^2 s^{-1}	(7)	Jain et al. (2017)

We ran a large suite of models (~10^4) where planetary gravity (as a proxy for planetary mass), surface temperature (for instellation and/or surface climate conditions), mantle interior temperature, and lithospheric age (which, along with mantle and surface temperature, dictates heat flow) were randomly drawn from uniform distributions. Our values for surface gravitational acceleration, g, spanned 5–40 m s^{-2}, corresponding to a rocky world of about half the mass of Earth (assuming a comparable density) to a super-Earth of substantially greater density than our own planet, for example, Kepler-406 c (Marcy et al., 2014). To encompass a broad range of star–planet distances, stellar types, and planetary climatic conditions, we considered surface temperatures, T_s, of 200–1,000 K. We also took lithosphere ages, t, of 5–300 Myr, encompassing the mean age of oceanic crust on Earth of about 64 Myr (Seton et al., 2020), as well as all but the very oldest ocean floor (Granot, 2016); mantle interior temperatures, T_m, of 1,500–2,000 K; strain rates of 10^{-13}, 10^{-14}, 10^{-15}, and 10^{-16} s^{-1}; and considered cases where $p = 0.5$, $q = 2$ and where $p = 1$, $q = 2$, as well as cases where pore pressure is hydrostatic and where $P_f = 0$. We summarize the parameters used in our models in Table 1.

3. Results

We find that planetary mass, surface temperature, and lithospheric age all impact the maximum depth of the BDT, whereas the influence of mantle interior temperature is negligible (Figure 1 and Figures S1–S3 in Supporting Information S1). With increasing gravity because of greater planetary mass, the stress required

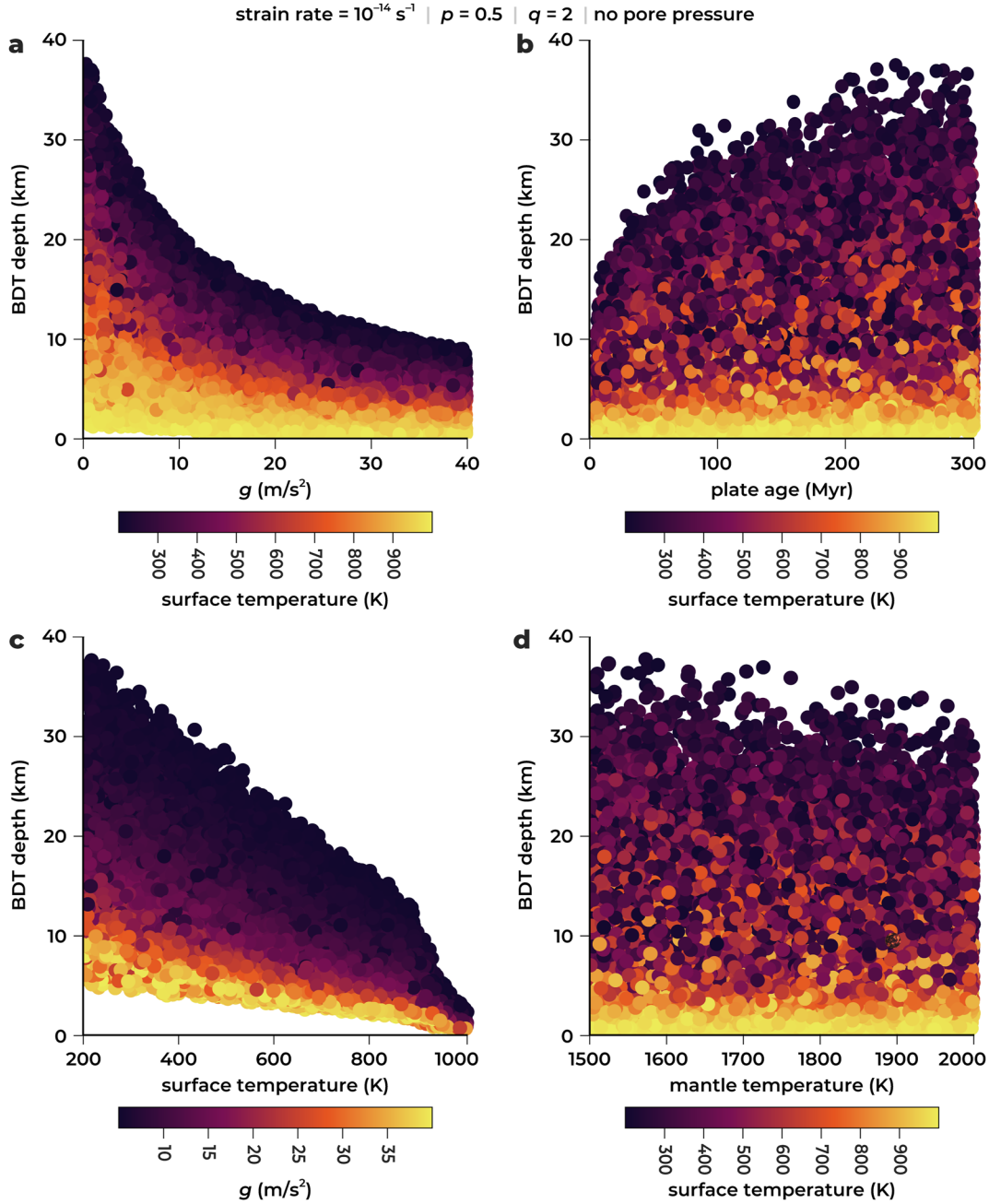

Figure 1. Modeled brittle-ductile transition (BDT) depths. Each symbol represents one model calculation for a strain rate of 10^{-14} s^{-1}, with $p = 0.5$ and $q = 2$, and no pore pressure on faults (i.e., for a hot and dry planetary surface). (a) BDT depth as a function of surface gravitational acceleration, g, and colored by surface temperature, T_s. (b) BDT depth as a function of lithosphere (and thus planetary) age, t, again colored by T_s. (c) BDT depth as a function of T_s, with model symbols colored by (g). (d) BDT depth as a function of mantle temperature, T_m, with symbols colored by T_s.

for frictional sliding (i.e., brittle failure) increases more sharply with depth than for lower gravity values. The stress needed to drive viscous flow is not so strongly affected, as this value depends much more on temperature than on pressure. As a result, the intersection of these two stress curves shifts to shallower depths as g increases (Figure 1a). For a representative strain rate of 10^{-14} s^{-1}, BDT depth ranges from <1 km to ≈30 km when $g = 5$ m s^{-2}; this spread is controlled by the other factors we varied (primarily T_s and t). At the other end of our range of gravity values, with $g = 40$ m s^{-2}, the BDT depth varies from <1 km to ≈10 km.

Varying lithospheric age, t, returns a similar trend. Lithospheric age roughly scales with planet age. A younger planetary body will, generally speaking, have higher interior temperatures because of heat produced by long- (i.e., K–U–Th) and short- (i.e., ^{26}Al) lived radionuclides, more residual kinetic energy acquired during accretion, more vigorous mantle convection, and hence a thinner lithosphere with a lower effective cooling age. With secular cooling, lithospheric thickness and hence the effective cooling age of the lithosphere generally increases. The younger the lithosphere, the steeper the geotherm; this configuration sees the stress needed for viscous flow decrease more sharply with depth, because of warmer temperatures, than is the case for older, colder lithosphere. The stress required for frictional sliding, however, is unaffected. Accordingly, the younger (or thinner) the lithosphere, the shallower the BDT depth (Figure 1b). With an age of $t = 5$ Myr and a strain rate again of 10^{-14} s^{-1}, we calculated a range of BDT maxima from <1 km to ≈15 km; with an age of $t = 300$ Myr, this depth extent increases to as much as ≈40 km.

Yet it is surface temperature that exerts the strongest control on BDT depth (Figure 1c). Higher model surface temperatures are reflected in hotter lithospheres generally, for all plate ages or planetary masses, and thus lower viscous stresses at all depths. Again, as the stress required for frictional sliding is not sensitive to temperature, the lower viscous stress means that the BDT becomes shallower for higher values of T_s. With a representative strain rate once more of 10^{-14} s^{-1}, the BDT extends from ∼5 to 40 km at a surface temperature of 200 K (Figure 1c). When T_s is 1,000 K, however, *all* of our models show BDT depths ≤5 km—even for low surface gravity values (Figure 1a) and/or old, cold, thick lithospheres (Figure 1b). Finally, our models indicate that mantle interior temperature does not play a large role in controlling the depth of the BDT (Figure 1d).

The trends described above also apply for models where $p = 1$ instead of $p = 0.5$, when fault fluid pressure was assumed to be hydrostatic, and for models featuring different strain rates (Figures S1–S3 in Supporting Information S1). Models with $p = 1$ show decreased ductile strength, all other factors held equal, hence leading to relatively shallower BDT depths. However, this effect is small, especially at high surface temperatures and with high surface gravity, such that differences in BDT depth for a given set of parameters when $p = 1$ compared with $p = 0.5$ are typically <1 km (Figure S1 in Supporting Information S1). With hydrostatic pore pressure, the BDT shifts deeper because fault strength increases more shallowly with depth; indeed, the depth to the BDT can increase by as much as 5–10 km for low values of surface temperature and gravitational acceleration (compare Figures S2a and S2b in Supporting Information S1, and Figures S2c and S2d in Supporting Information S1). However, for high surface temperatures and gravity, the differences between models with hydrostatic pore pressure and those with no fluid pore pressure shrink to 1 km or less. Moreover, planets with high surface temperatures are unlikely to have hydrated faults because of a lack of liquid surface or groundwater in the first place. And ductile rock strength increases with strain rate, as higher differential stress is required to drive flow. As a result, BDT depths shift deeper with increasing strain rates (Figure S3 in Supporting Information S1).

4. Discussion

Deeper BDT zones (and thus greater brittle lithosphere thicknesses) are generally seen for older and/or smaller planets (i.e., relatively high t and/or relatively low g); the inverse set of factors predicts shallower BDTs and thus thinner brittle lithospheres (Figure 1 and Figures S1–S3 in Supporting Information S1). However, of the three factors we modeled here, surface temperature clearly exerts the strongest control: very high surface temperatures lead to shallow BDTs, regardless of t or g (Figure 1c).

Our models are not sensitive to *why* a planet's surface temperature is high. Such a condition might result from external and/or internal factors. The former category includes the effects of incident stellar radiation, as a function of distance to a planet's host star and/or the energy output of that star. An extreme example of high T_s because of instellation is 55 Cancri e, a super-Earth with an orbital semi-major axis of 2.3 million km (Bourrier et al., 2018), and thus an estimated surface equilibrium temperature, T_{eq}, of 1958 K (Demory et al., 2011). (Here, T_{eq} is the corresponding surface temperature of a black body at that orbital distance heated by instellation alone.) Internal factors include the role of climate on T_s. In this regard, Venus and even Earth offer useful illustrations: T_{eq} values for these worlds are 227 and 254 K, respectively, yet the greenhouse effect drives corresponding mean surface temperatures to 737 K for Venus and 287 K for Earth.

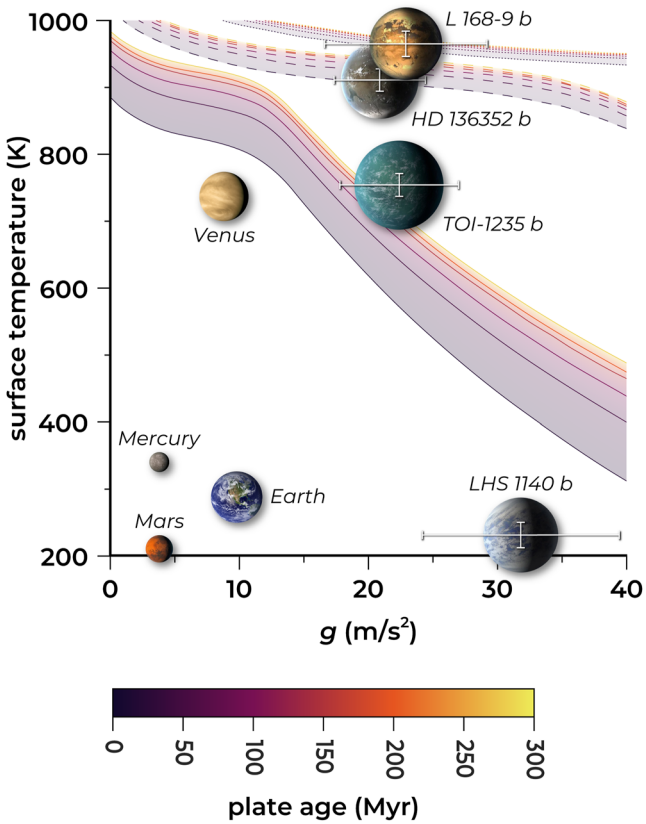

Figure 2. A plot of brittle lithospheric thickness as a function of surface gravitational acceleration, g, surface temperature, T, and plate age (as a proxy for heat flow). The four planets of the inner Solar System are shown, as are four super-Earths for which radius, mass, and equilibrium temperatures are available: HD 136352 b, L 168-9 b, LHS 1140 b, and TOI-1235 b. The ranges of uncertainty in g and T for the exoplanets are shown with white lines. All planets are shown to scale; the illustrations of the four exoplanets are artistic impressions. The solid, dashed, and dotted lines denote where on this plot brittle lithosphere thickness is 5, 2, and 1 km for a range of plate ages from 0 to 300 Myr.

Importantly, the maximum temperature we consider is 1000 K; whether the result of instellation, climate, or both, basaltic rock is still solid at that temperature, unlike for 55 Cancri e—even if the confluence of g, T_s, or t results in a prediction of ductile deformation.

We show the confluence in Figure 2, where these three variables are plotted. Interestingly, there are particular combinations of these planetary properties where our models predict brittle lithosphere thickness to be remarkably low; we delineate the parameter space for brittle lithospheres as thin as 5 km, 2 km, and 1 km with solid, dashed, and dotted lines, respectively, color-coded by plate age in Figure 2. The relative positions of the four inner Solar System planets are shown, as are four super-Earths for which surface gravity and surface temperature estimates are currently available: HD 136352 b (Kane et al., 2020), L 168-9 b (Astudillo-Defru et al., 2020), LHS 1140 b (Dittman et al., 2017), and TOI-1235 b (Cloutier et al., 2020). LHS 1140 b does not plot within these bounds but, per our models, TOI-1235 b, HD 136352 b, and L 168-9 b have brittle lithospheres no more than about 5 km thick (Figure 2).

This finding raises the prospect of what we term here "eggshell planets," worlds where the outer brittle layer is sufficiently thin—because of some combination of surface temperature, planetary mass, and heat flux—that almost all of the lithosphere deforms in a ductile manner. This interior mechanical structure has meaningful geological consequences. For example, such thin brittle lithospheres might not have sufficient flexural rigidity to support high-standing topography, as is seen in oceanic settings on Earth where volcanic loads down-flex relatively thin brittle oceanic lithosphere (e.g., Luis & Neves, 2006). Our models indicate that the lithospheric strength of both HD 136352 b and L 168-9 b is substantially less than that of worlds with thicker brittle lithospheres such as, for example, Earth and Mars (Figure 3).

It is unclear to what extent Earth-like plate tectonics might operate on eggshell planets. That process requires both that mantle forces can overcome the strength of the lithosphere, and that the lithosphere is strong and dense enough to subduct (e.g., Bercovici & Ricard, 2014). Additionally, both water (Solomatov, 2004a, b; Korenaga, 2010) and cool surface temperatures (e.g., Foley et al., 2012; Lenardic et al., 2008) have been proposed as critical enablers of plate tectonics. Surface water can reduce lithospheric strength by lubricating faults (Kohlstedt et al., 1995; Stesky, 1978), and interior water weakens viscously flowing mantle (e.g., Hirth & Kohlstedt, 2003). Low surface temperatures can promote plate tectonics by increasing convective stresses in the lithosphere, thus making it more prone to yielding (Lenardic, 2018), as well as by suppressing grain growth in the lithosphere such that weak plate boundaries can more readily form via grain-size reduction (Foley et al., 2012). We find that very thin brittle lithospheres require surface temperatures in excess of 700 K, however (Figure 2). It may be, then, that thin brittle layers and a lack of plate tectonics are not cause and effect, but simply two consequences of a rocky planet with a high surface temperature.

Yet eggshell planets might not be in the stagnant lid tectonic regime, either. Numerical modeling of mantle convection with high intrusion efficiencies yields a "plutonic-squishy lid" tectonic regime, characterized by both vertical and horizontal motions of small, strong, but ephemeral plates (Lourenço et al., 2020). This tectonic state may be applicable to modern Venus, where the high mean surface temperature leads to predictions of a relatively thin brittle lithosphere, at least for the lowlands (e.g., Buck, 1992; Ghail, 2015).

The cycling of volatiles into the Venus interior today is likely limited to crustal delamination (Elkins-Tanton et al., 2007) and spatially localized subduction (Davaille et al., 2017), and so takes place at a much

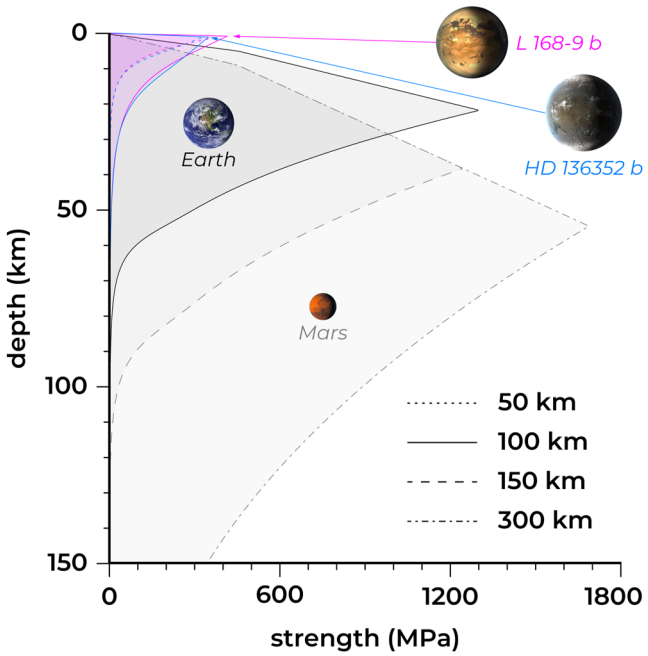

Figure 3. A plot of calculated lithospheric strength versus depth for Earth (black envelope) and Mars (gray), as well as two "eggshell" super-Earths: L 168-9 b and HD 136352 b (pink and blue envelopes, respectively). The profile for Earth is for a total lithospheric thickness of 100 km (solid line), with the bottom of the brittle-ductile transition (BDT) at a depth of approximately 25 km. Total lithospheric thicknesses of 150 km (dashed line) and 300 km (dashed-dotted line) are shown for Mars; here, the corresponding maximum BDT values are ~40 and ~60 km, respectively. For L 168-9 b and HD 136352 b, total lithospheric thicknesses of 50 km (dotted lines) and 100 km (solid lines) are shown; corresponding maximum BDT depth values are but a few km for both. The strengths of the super-Earth lithospheres at the maximum BDT are substantially lower than those of Earth and Mars. The total lithospheric thicknesses here are the thicknesses of the assumed conductive thermal boundary layers where temperature follows an error function; this approach offers a rough approximation for BDT depth on stagnant-lid Mars. All planets are shown to scale; the illustrations of the two exoplanets are artistic impressions.

lower rate than on Earth. Without surface water, any physical or chemical weathering on Venus in the current epoch is anhydrous (Zolotov, 2018) and there is little prospect for CO_2 drawdown; this must be the case for eggshell planets, too, especially given that high T_s reduces weathering rates (Hakim et al., 2021). Indeed, limited topography such as that in the Venus lowlands also impedes weathering: lower relief means less erosion, and thus a proportionately longer time to expose fresh surfaces for weathering. If the Venus lowlands are representative of eggshell planet surfaces generally, then we might reasonably infer that such exoplanets have widespread, distributed volcanic and tectonic activity (cf. Solomon et al., 1992), little elevated topography, and limited volatile cycling and chemical weathering.

5. Concluding Remarks

This study offers a framework for predicting brittle lithospheric thickness on rocky exoplanets for which estimates of mass, radius, and surface temperature are available. Per our results, those with very thin brittle layers (i.e., ≤5 km thick) are likely to be super-Earths that are geologically young and/or have elevated radiogenic element abundances relative to Earth, and are close to their stars and/or are runaway greenhouses. In turn, worlds that are smaller, older, and/or more distant from their host star probably have thicker brittle lithospheres. The interplay between these parameters is complex, but the surface temperature is the primary determinant of brittle lithospheric thickness.

Of course, our study is necessarily simplistic, since we have essentially no geological observations of exoplanets with which to constrain our parameter space. We assume here that exoplanets have peridotitic mantles and basaltic crusts, and implicitly treat lithospheric age as a measure for heat flux. Yet the ranges for g and T_s we consider encompass those of the inner Solar System planets and some of the largest known rocky exoplanets; our heat flux and strain rates span two and four orders of magnitude, respectively.

A key prediction we make here is that so-called eggshell planets will have little elevated topography. This prediction can be tested with future generations of telescopes capable of searching for constructional or orogenic topography on exoplanets (Landais et al., 2019; McTier & Kipping, 2018), particularly on TOI-1235 b, HD 136352 b, and L 168-9 b (per our Figure 2). Models for exoplanet tectonic regimes, such as the hemispherical mode proposed for LHS 3844 b (Meier et al., 2021), can now incorporate the effects of brittle lithospheric thickness in addition to lithospheric strength (Figure 3). Finally, very thin brittle layers have implications for the distribution and character of a planet's volcanic and tectonic activity, and for its ability to recycle volatiles. Eggshell planets are more likely to host distributed volcanism akin to the Venus lowlands rather than having such activity concentrated along plate boundaries, as is the case for Earth. And, with limited volatile cycling and reduced chemical fluxing associated with weathering compared with Earth, such worlds may have CO_2-rich and N-poor atmospheres (Mikhail & Sverjensky, 2014; Sleep and Zahnle, 2001), as Venus and Mars do. As more super-Earths are discovered that satisfy the definition of an eggshell planet, they will join TOI-1235 b, HD 136352 b, and L 168-9 b as strong candidates for atmospheric characterization with planned large-aperture telescopes such as the James Webb Space Telescope.

Data Availability Statement

Our research here made use of NASA's Planetary Data System and Astrophysics Data System. The MATLAB code for calculating brittle-ductile transition depths on planets as a function of surface gravity, mantle temperature, surface temperature, and lithosphere thickness (Foley, 2021a), as well as the models we calculated (Foley, 2021b), are available on Zenodo.

Acknowledgments
P. K. Byrne acknowledges support from North Carolina State University. Funding for S. Mikhail was provided by NERC standard grant NE/PO12167/1 and UK Space Agency Aurora grant ST/T001763/1. M. J. Heap thanks the Institut Universitaire de France (IUF) for support. The authors thank Jun Korenaga and Shintaro Azuma for constructive comments that improved this manuscript.

References

Astudillo-Defru, N., Cloutier, R., Wang, S. X., Teske, J., Brahm, R., Hellier, C., et al. (2020). A hot terrestrial planet orbiting the bright M dwarf L 168-9 unveiled by TESS. *Astronomy and Astrophysics*, *636*(A58). https://doi.org/10.1051/0004-6361/201937179

Bercovici, D., & Ricard, Y. (2014). Plate tectonics, damage and inheritance. *Nature*, *508*, 513–516. https://doi.org/10.1038/nature13072

Beuthe, M. (2010). East-west faults due to planetary contraction. *Icarus*, *209*, 795–817. https://doi.org/10.1016/j.icarus.2010.04.019

Bourrier, V., Lecavelier des Etangs, A., Ehrenreich, D., Sanz-Forcada, J., Allart, R., Ballester, G. E., et al. (2018). *Hubble* PanCET: An extended upper atmosphere of neutral hydrogen around the warm Neptune GJ 3470b. *Astronomy and Astrophysics*, *620*, A147. https://doi.org/10.1051/0004-6361/201833675

Buck, R. W. (1992). Global decoupling of crust and mantle: Implications for topography, geoid and mantle viscosity on Venus. *Geophysical Research Letters*, *19*, 2111–2114. https://doi.org/10.1029/92GL02462

Byerlee, J. (1978). Friction of rocks. *Pure and Applied Geophysics*, *116*, 615–626. https://doi.org/10.1007/BF00876528

Byrne, P. K. (2019). A comparison of inner solar system volcanism. *Nature Astronomy*, *4*, 321–327. https://doi.org/10.1038/s41550-019-0944-3

Byrne, P. K., Klimczak, C., Şengör, A. M. C., Solomon, S. C., Watters, T. R., & Hauck, S. A. (2014). Mercury's global contraction much greater than earlier estimates. *Nature Geoscience*, *7*, 301–307. https://doi.org/10.1038/ngeo2097

Campante, T. L., Barclay, T., Swift, J. J., Huber, D., Adibekyan, V. Z., Cochran, W., et al. (2015). An ancient extrasolar system with five sub-Earth-size planets. *The Astrophysical Journal*, *799*, 2. https://doi.org/10.1088/0004-637X/799/2/170

Cloutier, R., Rodriguez, J. E., Irwin, J., Charbonneau, D., Stassun, K., Mortier, A., et al. (2020). TOI-1235 b: A keystone super-Earth for testing radius valley emergence models around early M dwarfs. *The Astronomical Journal*, *160*, 22. https://doi.org/10.3847/1538-3881/ab9534

Comer, R. P., Solomon, S. C., & Head, J. W. (1985). Mars: Thickness of the lithosphere from the tectonic response to volcanic loads. *Reviews of Geophysics*, *23*, 61–92. https://doi.org/10.1029/RG023i001p00061

Davaille, A., Smrekar, S. E., & Tomlinson, S. (2017). Experimental and observational evidence for plume-induced subduction on Venus. *Nature Geoscience*, *10*, 349–355. https://doi.org/10.1038/NGEO2928

Demory, B.-O., Gillon, M., Deming, D., Valencia, D., Seager, S., Benneke, B., et al. (2011). Detection of a transit of the super-Earth 55 Cancri e with warm *Spitzer*. *Astronomy and Astrophysics*, *533*, A114. https://doi.org/10.1051/0004-6361/201117178

Demouchy, S., Tommasi, A., Boffa Ballaran, T., & Cordier, P. (2013). Low strength of Earth's uppermost mantle inferred from tri-axial deformation experiments on dry olivine crystals. *Physics of the Earth and Planetary Interiors*, *220*, 37–49. https://doi.org/10.1016/j.pepi.2013.04.008

Dittman, J. A., Irwin, J. A., Charbonneau, D., Bonfils, X., Astudillo-Defru, N., Haywood, R. D., et al. (2017). A temperate rocky super-Earth transiting a nearby cool star. *Nature*, *544*, 333–336. https://doi.org/10.1038/nature22055

Egea-González, I., Ruiz, J., Fernández, C., Williams, J.-P., Márquez, Á., & Lara, L. M. (2012). Depth of faulting and ancient heat flows in the Kuiper region of Mercury from lobate scarp topography. *Planetary and Space Science*, *60*, 193–198. https://doi.org/10.1016/j.pss.2011.08.003

Elkins-Tanton, L. T., Smrekar, S. E., Hess, P. C., & Parmentier, E. M. (2007). Volcanism and volatile recycling on a one-plate planet: Applications to Venus. *Journal of Geophysical Research*, *112*, E04S06. https://doi.org/10.1029/2006JE002793

Foley, B. J. (2021a). *Brittle-ductile transition code*. Zenodo. https://doi.org/10.5281/zenodo.5560138

Foley, B. J. (2021b). *Brittle-ductile transition depth dataset*. Zenodo. https://doi.org/10.5281/zenodo.5560142

Foley, B. J., Bercovici, D., & Landuyt, W. (2012). The conditions for plate tectonics on super-Earths: Inferences from convection models with damage. *Earth and Planetary Science Letters*, *331–332*, 281–290. https://doi.org/10.1016/j.epsl.2012.03.028

Ghail, R. (2015). Rheological and petrological implications for a stagnant lid regime on Venus. *Planetary and Space Sciences*, *113–114*, 2–9. https://doi.org/10.1016/j.pss.2015.02.005

Granot, R. (2016). Palaeozoic oceanic crust preserved beneath the eastern Mediterranean. *Nature Geoscience*, *9*, 701–705. https://doi.org/10.1038/ngeo2784

Hakim, K., Bower, D. J., Tian, M., Deitrick, R., Auclair-Desrotour, P., Kitzmann, D., et al. (2021). Lithologic controls on silicate weathering regimes of temperate planets. *Planetary Science Journal*, *2*, 49. https://doi.org/10.3847/PSJ/abe1b8

Head, J. W., & Wilson, L. (1992). Lunar mare volcanism: Stratigraphy, eruption conditions, and evolution of secondary crusts. *Geochimica et Cosmochimica Acta*, *56*, 2155–2175. https://doi.org/10.1016/0016-7037(92)90183-J

Hirth, G., & Kohlstedt, D. (2003). Rheology of the upper mantle and the mantle wedge: A view from the experimentalists. *Geophysical Monograph Series*, *138*, 83–105. https://doi.org/10.1029/138GM06

Jain, C., & Korenaga, J. (2020). Synergy of experimental rock mechanics, seismology, and geodynamics reveals still elusive upper mantle rheology. *Journal of Geophysical Research*, *125*, e2020JB019896. https://doi.org/10.1029/2020JB019896

Jain, C., Korenaga, J., & Karato, S. (2017). On the yield strength of oceanic lithosphere. *Geophysical Research Letters*, *44*, 9716–9722. https://doi.org/10.1002/2017GL075043

Jain, C., Korenaga, J., & Karato, S. (2019). Global analysis of experimental data on the rheology of olivine aggregates. *Journal of Geophysical Research*, *124*, 310–334. https://doi.org/10.1029/2018JB016558

Kane, S. R., Yalçınkaya, S., Osborn, H. P., Dalba, P. A., Nielson, L. D., Vanderburg, A., et al. (2020). Transits of known planets orbiting a naked-eye star. *The Astronomical Journal*, *160*, 129. https://doi.org/10.3847/1538-3881/aba835

Katayama, I. (2021). Strength models of the terrestrial planets and implications for their lithospheric structure and evolution. *Progress in Earth and Planetary Science*, *8*, 1. https://doi.org/10.1186/s40645-020-00388-2

Klimczak, C., Byrne, P. K., Şengör, A. M. C., & Solomon, S. C. (2019). Principles of structural geology on rocky planets. *Canadian Journal of Earth Sciences*, *56*, 1437–1457. https://doi.org/10.1139/cjes-2019-0065

Kohlstedt, D. L., Evans, B., & Mackwell, S. J. (1995). Strength of the lithosphere: Constraints imposed by laboratory experiments. *Journal of Geophysical Research*, *100*, 17587–17602. https://doi.org/10.1029/95JB01460
Kohlstedt, D. L., & Mackwell, S. J. (2010). Strength and deformation of planetary lithospheres. In T. Watters, & R. Schultz (Eds.), *Planetary tectonics* (pp. 397–456). Cambridge University Press. https://doi.org/10.1017/CBO9780511691645.010
Korenaga, J. (2010). On the likelihood of plate tectonics on super-Earths: Does size matter? *The Astrophysical Journal Letters*, *725*, L43–L46. https://doi.org/10.1088/2041-8205/725/1/L43
Korenaga, J. (2017). Pitfalls in modeling mantle convection with internal heat production. *Journal of Geophysical Research*, *122*, 4064–4085. https://doi.org/10.1002/2016JB013850
Korenaga, J. (2020). Plate tectonics and surface environment: Role of the oceanic upper mantle. *Earth-Science Reviews*, *205*, 103185. https://doi.org/10.1016/j.earscirev.2020.103185
Kreidberg, L., Koll, D. D. B., Morley, C., Hu, R., Schaefer, L., Deming, D., et al. (2019). Absence of a thick atmosphere on the terrestrial exoplanet LHS 3844b. *Nature*, *273*, 87–90. https://doi.org/10.1038/s41586-019-1497-4
Kumamoto, K. K., Thom, C. A., Wallis, D., Hansen, L. N., Armstrong, D. E., Warren, J. M., et al. (2017). Size effects resolve discrepancies in 40 years of work on low-temperature plasticity in olivine. *Science Advances*, *3*(9), e1701338. https://doi.org/10.1126/sciadv.1701338
Landais, F., Schmidt, F., & Lovejoy, S. (2019). Topography of (exo)planets. *Monthly Notices of the Royal Astronomical Society*, *484*, 787–793. https://doi.org/10.1093/mnras/sty3253
Lenardic, A. (2018). The diversity of tectonic modes and thoughts about transitions between them. *Philosophical Transactions of the Royal Society A*, *376*, 20170416. https://doi.org/10.1098/rsta.2017.0416
Lenardic, A., Jellinek, A. M., & Moresi, L.-N. (2008). A climate induced transition in the tectonic style of a terrestrial planet. *Earth and Planetary Science Letters*, *271*, 34–42. https://doi.org/10.1016/j.epsl.2008.03.031
Lourenço, D. L., Rozel, A. B., Ballmer, M. D., & Tackley, P. J. (2020). Plutonic-squishy lid: A new global tectonic regime generated by intrusive magmatism on earth-like planets. *Geochemistry, Geophysics, Geosystems*, *21*, e2019GC008756. https://doi.org/10.1029/2019GC008756
Luis, J. F., & Neves, M. C. (2006). The isostatic compensation of the Azores Plateau: A 3D admittance and coherence analysis. *Journal of Volcanology and Geothermal Research*, *156*, 10–22. https://doi.org/10.1016/j.jvolgeores.2006.03.010
Marcy, G. W., Isaacson, H., Howard, A. W., Rowe, J. F., Jenkins, J. M., Bryson, S. T., et al. (2014). Masses, radii, and orbits of small Kepler planets: The transition from gaseous to rocky planets. *Astronomical Journal Supplement Series*, *210*, 20. https://doi.org/10.1088/0067-0049/210/2/20
McGovern, P. J., Solomon, S. C., Smith, D. E., Zuber, M. T., Simons, M., Wieczorek, M. A., et al. (2004). Correction to "Localized gravity/topography admittance and correlation spectra on Mars: Implications for regional and global evolution". *Journal of Geophysical Research*, *109*, E07007. https://doi.org/10.1029/2004JE002286
McGovern, P. J., Solomon, S. C., Smith, D. E., Zuber, M. T., Simons, M., Wieczorek, M. A., et al. (2002). Localized gravity/topography admittance and correlation spectra on Mars: Implications for regional and global evolution. *Journal of Geophysical Research*, *107*(E12), 5136. https://doi.org/10.1029/2002JE001854
McTier, M. A. S., & Kipping, D. M. (2018). Finding mountains with molehills: The detectability of exotopography. *Monthly Notices of the Royal Astronomical Society*, *475*, 4978–4985. https://doi.org/10.1093/mnras/sty143
Meier, T. G., Bower, D. J., Lichtenberg, T., Tackley, P. J., & Demory, B.-O. (2021). Hemispheric tectonics on super-Earth LHS 3844b. *The Astrophysical Journal Letters*, *908*, L48. https://doi.org/10.3847/2041-8213/abe400
Mikhail, S., & Heap, M. J. (2017). Hot climate inhibits volcanism on Venus: Constraints from rock deformation experiments and argon isotope geochemistry. *Physics of the Earth and Planetary Interiors*, *268*, 18–34. https://doi.org/10.1016/j.pepi.2017.05.007
Mikhail, S., & Sverjensky, D. A. (2014). Nitrogen speciation in upper mantle fluids and the origin of Earth's nitrogen-rich atmosphere. *Nature Geoscience*, *7*, 816–819. https://doi.org/10.1038/NGEO2271
Montési, L. G. J. (2013). Fabric development as the key for forming ductile shear zones and enabling plate tectonics. *Journal of Structural Geology*, *50*, 254–266. https://doi.org/10.1016/j.jsg.2012.12.011
Mulyukova, E., & Bercovici, D. (2017). Formation of lithospheric shear zones: Effect of temperature on two-phase grain damage. *Physics of the Earth and Planetary Interiors*, *270*, 195–212. https://doi.org/10.1016/j.pepi.2017.07.011
O'Neill, C., Jellinek, A. M., & Lenardic, A. (2007). Conditions for the onset of plate tectonics on terrestrial planets and moons. *Earth and Planetary Science Letters*, *261*(1–2), 20–32. https://doi.org/10.1016/j.epsl.2007.05.038
O'Neill, C., & Lenardic, A. (2007). Geological consequences of super-sized Earths. *Geophysical Research Letters*, *34*, 19. https://doi.org/10.1029/2007GL030598
Peterson, G. A., Johnson, C. L., Byrne, P. K., & Phillips, R. J. (2020). Fault structure and origin of compressional tectonic features within the smooth plains on Mercury. *Journal of Geophysical Research Planets*, *125*, e2019JE006183. https://doi.org/10.1029/2019JE006183
Phillips, R. J., Johnson, C. L., Mackwell, S. J., Morgan, P., Sandwell, D. T., & Zuber, M. T. (1997). Lithospheric mechanics and dynamics of Venus. In S. W. Bougher, D. M. Hunten, & R. J. Phillips (Eds.), *Venus II* (pp. 1163–1204). University of Arizona Press.
Seton, M., Müller, R. D., Zahirovic, S., Williams, S., Wright, N. M., Cannon, J., et al. (2020). A global data set of present-day oceanic crustal age and seafloor spreading parameters. *Geochemistry, Geophysics, Geosystems*, *21*, e2020GC009214. https://doi.org/10.1029/2020GC009214 10.1029/2020gc009214
Sleep, N. H., & Zahnle, K. (2001). Carbon dioxide cycling and implications for climate on ancient Earth. *Journal of Geophysical Research*, *106*, 1373–1399. https://doi.org/10.1029/2000JE001247
Solomatov, V. S. (2004a). Initiation of subduction by small-scale convection. *Journal of Geophysical Research*, *109*, B01412. https://doi.org/10.1029/2003JB002628
Solomatov, V. S. (2004b). Correction to "Initiation of subduction by small-scale convection". *Journal of Geophysical Research*, *109*, B05408. https://doi.org/10.1029/2004JB003143
Solomon, S. C., & Head, J. W. (1980). Lunar mascon basins: Lava filling, tectonics, and evolution of the lithosphere. *Reviews of Geophysics and Space Physics*, *18*, 107–141. https://doi.org/10.1029/RG018i001p00107
Solomon, S. C., Smrekar, S. E., Bindschadler, D. L., Grimm, R. E., Kaula, W. M., McGill, G. E., et al. (1992). Venus tectonics: An overview of Magellan observations. *Journal of Geophysical Research*, *97*, 13199–13255. https://doi.org/10.1029/92JE01418
Stein, C., Finnenkötter, A., Lowman, J. P., & Hansen, U. (2011). The pressure-weakening effect in super-Earths: Consequences of a decrease in lower mantle viscosity on surface dynamics. *Geophysical Research Letters*, *38*, L21201. https://doi.org/10.1029/2011GL049341
Stern, R. J., Gerya, T., & Tackley, P. J. (2018). Stagnant lid tectonics: Perspectives from silicate planets, dwarf planets, large moons, and large asteroids. *Geoscience Frontiers*, *9*, 103–119. https://doi.org/10.1016/j.gsf.2017.06.004
Stesky, R. M. (1978). Rock friction-effect of confining pressure, temperature, and pore pressure. *Pure and Applied Geophysics*, *116*, 690–704. https://doi.org/10.1007/BF00876532

Strom, R. G., Trask, N. J., & Guest, J. E. (1975). Tectonism and volcanism on Mercury. *Journal of Geophysical Research*, *80*, 2478–2507. https://doi.org/10.1029/JB080i017p02478

Suppe, J., & Connors, C. (1992). Critical taper wedge mechanics of fold-and-thrust belts on Venus' initial results from Magellan. *Journal of Geophysical Research*, *97*, 13545–13561. https://doi.org/10.1029/92JE01164

Surkov, Y. A., Moskalyeva, L. P., Scheglov, O. P., Kharyukova, V. P., Manvelyan, O. S., Kirichenko, V. S., & Dudin, A. D. (1983). Determination of the elemental composition of rocks on Venus by Venera 13 and Venera 14 (preliminary results). *Journal of Geophysical Research*, *88*, A481–A493. https://doi.org/10.1029/JB088iS02p0A481

Tanaka, K. L., Skinner, J. A., Jr., Dohm, J. M., Irwin, R. P., III, Kolb, E. J., Fortezzo, C. M., et al. (2014). Geologic Map of Mars: U.S. Geological Survey Scientific Investigations Map 3292, scale 1:20,000,000 pamphlet (USGS). https://doi.org/10.3133/sim3292

Turcotte, D. L., & Schubert, G. (2002). *Geodynamics* (2nd ed., p. 456). Cambridge University Press.

Turcotte, D. L., Willemann, R. J., Haxby, W. F., & Norberry, J. (1981). Role of membrane stresses in the support of planetary topography. *Journal of Geophysical Research*, *86*, 3951–3959. https://doi.org/10.1029/JB086iB05p03951

Valencia, D., O'Connell, R. J., & Sasselov, D. D. (2007). Inevitability of plate tectonics on super-Earths. *The Astrophysical Journal*, *670*, L45–L48. https://doi.org/10.1086/524012

van Heck, H. J., & Tackley, P. J. (2011). Plate tectonics on super-Earths: Equally or more likely than on Earth. *Earth and Planetary Science Letters*, *310*, 252–261. https://doi.org/10.1016/j.epsl.2011.07.029

Violay, M., Gibert, B., Mainprice, D., Evans, B., Dautria, J.-M., Azais, P., & Pezard, P. (2012). An experimental study of the brittle-ductile transition of basalt at oceanic crust pressure and temperature conditions. *Journal of Geophysical Research*, *117*, B03123. https://doi.org/10.1029/2011JB008884

Warren, J. M., & Hirth, G. (2006). Grain size sensitive deformation mechanisms in naturally deformed peridotites. *Earth and Planetary Science Letters*, *248*, 438–450. https://doi.org/10.1016/j.epsl.2006.06.006

Yoder, H. S., Jr., & Tilley, C. E. (1962). Origin of basalt magmas: An experimental study of natural and synthetic rock systems. *Journal of Petrology*, *3*, 342–532. https://doi.org/10.1093/petrology/3.3.342

Zolotov, M. (2018). Chemical weathering on Venus. *Oxford Research Encyclopedia on Planetary Science*. https://doi.org/10.1093/acrefore/9780190647926.013.146